A simple way to improve anatomical mapping of functional brain imaging.

Nicolas Villain, Brigitte Landeau, Mathilde Groussard, Katell Mevel, Marine Fouquet, Jacques Dayan, Francis Eustache, Béatrice Desgranges, Gaël Chételat

A simple way to improve anatomical mapping of functional brain imaging

Nicolas Villain [1] , Brigitte Landeau [1] , Mathilde Groussard [1] , Katell Mevel [1] , Marine Fouquet [1] , Jacques Dayan [1 2] , Francis Eustache [1] , Béatrice Desgranges [1] , Gaël Chételat [1 *]

[1] Neuropsychologie cognitive et neuroanatomie fonctionnelles de la mémoire INSERM : U923 , EPHE , CHU Caen , Université de Caen , Cyceron, Bd Henri Becquerel, BP5229, 14074 Caen Cedex 5,FR

[2] Unité de Psychiatrie Périnatale CHU Caen , Service de Psychiatrie de l'Enfant et de l'Adolescent Avenue Clémenceau, Caen,FR

* Correspondence should be adressed to: Gaël Chételat <chetelat@cyceron.fr >

Abstract

Background and purpose

Advances in functional neuroimaging studies have led to the need for improved anatomical precision to face with more and more specific challenges. Nevertheless, functional MRI (fMRI) suffers from geometrical distortions which limit the matching between functional and anatomical data necessary to interpret fMRI results. The 'FieldMap' method is the most widely used technique to correct for geometrical distortions but in some cases cannot be applied or provides unsatisfactory results. The objective of the present study is thus to provide a very simple alternative method for distortion correction and to demonstrate its efficiency.

Methods

This correction relies on the non-linear registration of Echo-Planar-Imaging (EPI) acquisitions onto their corresponding undistorted non-EPI T2Star volume, and was tested on two independent groups of subjects undertaking the same paradigm but scanned with distinct EPI sequences.

Results

This procedure was found to considerably decrease the mismatch between functional and anatomical data in both groups, as revealed through several quantitative and qualitative measures on both EPI volumes and activation maps.

Conclusion

The present study describes a simple, rapid, and easily implementable method to significantly improve neuroanatomical accuracy of fMRI results localization, which may be relevant for future neuroimaging studies.

Introduction

Functional MRI (fMRI) is now the most widely used technique for functional neuroimaging studies of the human brain. The anatomical interpretation of fMRI results, termed as "activations", almost systematically depends on their projection onto anatomical T1-MRI images. However, while the focus of pioneer fMRI studies did not require highly specific anatomical accuracy in the location of activations, parallel advances in human functional brain research and neuroimaging techniques have progressively led to the need for improved anatomical precision. As examples, recent fMRI investigations focused on the differential functional connectivity of sixteen subparts of the anterior cingulate gyrus1 , or aimed at highlighting the differential roles of the hippocampal subfields2 or of eight subregions of the left frontal inferior gyrus3 in memory and language functions, respectively.

Unfortunately, fMRI data suffer from geometrical distortions, whose intensity may vary according to the Echo-Planar Imaging (EPI) sequence and the brain region, but which anyway limit the anatomical accuracy of resulting fMRI findings. Thus, even with the most accurate EPI-to-T1 rigid coregistration, functional and anatomical images are imperfectly matched as they do not have the same shape. As a consequence, the anatomical interpretation of fMRI findings may be tricky since some findings, especially those located in brain regions suffering from high geometrical distortions (such as anterior brain areas), would appear mislocated onto the T1 image. Many illustrations of this issue can be found in the current literature, such as activations supposed to be located in the anterior cingulate cortex but that clearly appeared into the corpus callosum genu when superimposed onto T1 anatomical images (see Figure 2 .a, cluster A in Vanderwal et al. (2008)4 ; and Figures 4 and 5 from Margulies et al. (2007)1 , for instance). Although activations were not misinterpreted in these studies, these examples illustrate the potential gap between genuine and apparent locations of activations that may blur fMRI data interpretations and limit current and future investigations. Besides, recently emerging multi-modal voxel-based neuroimaging studies5 as well as tools specifically designed for direct voxel-based comparisons between fMRI and morphometry (VBM) data6 , further stress on the need for an accurate matching between functional and anatomical MRI data.

Although still only occasionally applied, different methods have been proposed to correct for geometrical distortions, the most-widely used being the 'FieldMap' procedure7 ,8 . This method relies on a measured field map for the object inside the scanner to compute the existing distortions in the EPI images according to the relationships between spatial distortion and field inhomogeneity thanks to specific algorithms. This procedure depends upon the acquisition of two non-EPI T2 Star images with different echo time. It seems of interest to propose an alternative method that could be used in situations where field maps have not, or cannot, be collected or when the 'FieldMap' method fails to provide correct field map estimation.

Our purpose with this study is thus to propose an alternative method very simple to implement as it only relies on a single non-EPI T2 Star image and on algorithms widely implemented and already used in most neuroimaging laboratories. This method is based on roughly warping distorted EPI data onto corresponding undistorted non-EPI T2 Star image. This procedure was tested on two independent groups of subjects undertaking the same paradigm but scanned with distinct EPI sequences showing different sensitivity to geometrical distortions.

Materials & Methods

Participants

Twenty-four right-handed native French-speaking participants were included in our study (11 males; 13 females; mean age: 30.0±6.5). Subjects had no history of metabolic, psychiatric, serious head injury or neurological illness as confirmed by neurological clinical assessment. Signed informed consent was obtained prior to participation. The study was approved by the local ethical committee (CPP Nord-Ouest III) and was done in line with the declaration of Helsinki.

Design and Task

We designed an event-related self-referential paradigm known to consistently induce strong activations in the cortical midline structures including regions suffering from geometrical distortions such as the anterior cingulate gyrus and the medial prefrontal cortex9 –13 . Personality trait adjectives were successively presented to the subjects who had to indicate whether or not the adjective described either themselves (Self condition) or a personality (Other condition), or whether the adjective was positive or not (Semantic control condition). The personality was either the former French president Jacques Chirac (the experimentation started nine months after President Sarkozy election) or the famous French singer Johnny Hallyday, depending on the run. After a training session performed outside the scanner, subjects underwent two runs, each lasting 396 seconds and including 72 stimuli (12 positive Self , 12 negative Sel f, 12 positive Other , 12 negative Other , 12 positive Semantic , 12 negative Semantic). Each adjective was presented on a screen during 3500 ms together with a brief instruction on the nature of the judgment to perform (i.e. "Myself", "J. Chirac" or "J. Hallyday", and "Positive?", respectively corresponding to the Self , Other , and Semantic conditions), followed by a fixation cross of 1000 to 3000 ms (mean: 2000 ms). Order of presentation of the conditions was optimized using a Genetic Algorithm14 . Valence and length of the personality trait adjectives were rigorously counterbalanced across conditions. Finally, lists of adjectives displayed for each condition were also counterbalanced across subjects. Items were displayed using the E-Prime software (Psychology Software Tools, Pittsburgh, PA) implemented within IFIS System Manager (Invivo, Orlando, FL). Since the present study aimed at addressing methodological issues, only the Self and Semantic conditions were used in the following analyses. Indeed, this contrast is known to provide reliable and robust results across subjects, contrary to the Other condition4 ,9 –12 .

Data acquisition

A Philips (Eindhoven, The Netherlands) Achieva 3.0 T scanner from the GIP Cyceron (Caen, France) was used for data acquisition. For each participant, a high resolution T1-weighted anatomical image was first acquired using a 3D fast field echo sequence (3D-T1-FFE sagittal, TR=20 ms; TE=4.6 ms; flip angle=20°; 170 slices; slice thickness=1 mm; no gap; FoV=256×256 mm^2 ; matrix=256×256; in-plane resolution=1×1 mm^2), followed by a high resolution T2-weighted spin echo anatomical acquisition (2D-T2-SE sagittal, SENSE factor=2; TR=5500 ms; TE=80 ms; flip angle=90°; 81 slices; slice thickness=2 mm; no gap; FoV=256×256 mm^2 ; matrix=256×256; in-plane resolution=1×1 mm^2) and a non-EPI T2 Star image (2D-T2 Star-FFE axial, SENSE factor=2; TR=3505 ms; TE=30 ms; flip angle=90°; 70 slices; slice thickness=2 mm; no gap; FoV=256×256 mm^2 ; matrix=128×128; in-plane resolution=2×2 mm^2). Functional acquisitions of twelve subjects (6 males; mean age: 30.0±7.3) were done using an interleaved 2D T2 Star EPI sequence (2D-T2 Star-FFE-EPI axial, TR= 2200 ms; TE=35 ms; flip angle=80°; 35 slices; slice thickness=3.5 mm; no gap; matrix=64×64; FoV=224×224 mm^2 ; in-plane resolution= 3.5×3.5 mm^2 ; 185 volumes per run) termed as "standard EPI sequence" in what follows. Twelve additional subjects (5 males; mean age: 30.1±6.0) underwent an interleaved 2D T2 Star SENSE (SENSitivity Encoding) EPI sequence designed to reduce geometrical distortions by using parallel imaging, shorter echo time and smaller voxels (2D-T2 Star-FFE-EPI axial, SENSE factor=2; TR=2382 ms; TE=30 ms; flip angle=80°; 44 slices; slice thickness=2.8 mm; no gap; matrix=80×80; FoV=224×224 mm^2 ; in-plane resolution=2.8×2.8 mm^2 ; 172 volumes per run), and termed as the "SENSE EPI sequence".

Pre-processing and analysis of fMRI data

EPI data were first checked for the lack of artifacts through the creation of variance volume for each run and each subject, allowing to ensure that most signal variability was restricted to the cortex. We also applied TSDiffana (http://imaging.mrccbu.cam.ac.uk/imaging/DataDiagnostics) to each functional raw volume to confirm the lack of any isolated artifact into the images.

The pre-processing steps of fMRI data, detailed and illustrated in Figure 1 , were performed using SPM5 (Statistical Parametric Mapping; Wellcome Dept of Cognitive Neurology, London, UK) and applied to the two data samples with distinct EPI sequence. For each data set, two pre-processing procedures were applied, the first one corresponding to the standard pre-processing procedure while the second one included a supplementary step intended to reduce geometrical distortions.

Standard pre-processing procedure (Figure 1A and B)

After discarding the six first EPI volumes of each run (to allow for magnetic saturation effects), EPI volumes of each subject were corrected for slice timing and then realigned on the first volume of the first run. Individual T1-to-EPI rigid coregistration was then performed as followed: first, the mean EPI volume of each subject was rigidly coregistered onto the non-EPI T2Star acquisition; second, the non-EPI T2Star volume was rigidly coregistered onto the T2 image; and third the T2 volume was rigidly coregistered onto the T1 acquisition. The coregistration parameters resulting from these three steps were successively applied to all EPI volumes and those resulting from the third step were also applied to the non-EPI T2Star image (see Figure 1). The T1 image was then segmented/normalized using the SPM5 'Segment' procedure15 with the ICBM/MNI priors and the resulting parameters (of the so-called T1-to-MNI normalization) were applied to the coregistered T1, EPI, and non-EPI T2 Star volumes. Since the two data sets with distinct EPI sequences had different original spatial resolutions, differential smoothing was applied in order to obtain images of equivalent effective smoothness, and thus of identical resultant resolution5 ,16 . To this end, we used an isotropic Gaussian kernel of 7.72 mm FWHM for the standard EPI sequence, resulting in an effective smoothness identical to the SENSE EPI sequence images smoothed at 8 mm FWHM17 .

Additional EPI-to-non-EPI non-linear registration step (Figure 1C)

Non-EPI T2 Star volumes are not altered by geometrical distortion as they do not rely on a low bandwidth EPI acquisition, but they suffer from magnetic susceptibility artifacts since they are sensitive to the transverse magnetization decay of the signal measured with gradient echo sequences. Consequently, their global shape is a good approximate of the theoretical shape of undistorted EPI images. For this reason, we proposed here to correct for geometrical distortion by roughly warping distorted EPI images onto corresponding non-EPI T2 star image so that their global shape would tend to be similar to their theoretical undistorted one. Thus, after T1-to-EPI rigid coregistration, the mean EPI image was warped to roughly match the non-EPI T2 Star volume using the SPM5 'Normalize: Estimate' function (Source and Template images Smoothing: 4mm FWHM; Affine regularization: Average sized template). To avoid an extra-reslicing step as compared to the standard procedure, the so-called EPI-to-non-EPI warping parameters were combined to the T1-to-MNI normalization parameters described above, and applied to the coregistered T1, EPI, and non-EPI T2 Star volumes using the SPM5 'Deformation Toolbox'. Resulting images were finally smoothed as described above for the standard procedure.

Display of results and statistical analyses

First, in order to provide an overview of the warps induced by the EPI-to-non-EPI non-linear registration, warping parameters were transformed to jacobian determinants. The jacobian maps of each subject are first transformed (by subtracting one) so that negative values reflect expansion and positive values contractions, and then normalized onto MNI and smoothed at 8 mm FWHM. Areas of significant expansion (negative jacobians) and contraction (positive jacobians) were then assessed using a one-sample t-test for each EPI sequence group.

Second, in order to quantify the effect of the EPI-to-non-EPI non-linear registration step onto anatomical accuracy, we used the position of the most anterior voxel of the corpus callosum genu as an anatomical landmark. This landmark was selected because it is both expected to be concerned by geometrical distortion and easily identifiable on both T1 and EPI sequences. Indeed, due to magnetic susceptibility artifacts in EPI but not T1 images and to differences between T1 and EPI images in terms of intensity, resolution and contrast, we failed to find another reliable landmark that could be easily and accurately applied to both datasets. Thus, y and z MNI coordinates of the position of the most anterior voxel of the corpus callosum genu were obtained for each subject from the inter-hemispheric sagittal slice of the unsmoothed MNI-normalized T1, mean EPI, and mean EPI warped onto the non-EPI T2 Star volume. The Euclidian distances between the position of the corpus callosum genu in each of the two mean EPI images and that in the corresponding T1 volume were then calculated for each subject. These values were then entered in a 2×2 repeated-measures ANOVA including the 'pre-processing procedure' (with or without the EPI-to-non-EPI nonlinear registration step) as a repeated factor and the EPI sequence group (standard or SENSE) as a classification factor, and analyzed with the Statistica software (Statsoft, Tulsa, OK) to assess whether the additional EPI-to-non-EPI non-linear registration step significantly reduced the mismatch between anatomical and functional images.

Third, the effect of the additional EPI-to-non-EPI non-linear registration step was assessed onto activation maps. For this purpose, statistical analyses were conducted on functional images using SPM5 and the general linear model approach on a voxel-by-voxel basis with a random effects model implemented with a two-level procedure. Six different experimental conditions were modeled as δ functions at each stimulus onset according to the valence of the adjective (positive or negative) and the nature of judgment (Self , Other and Semantic). The ensuing hemodynamic response was modeled by convolving these δ functions with a canonical hemodynamic response function.

A single “Self minus Semantic ” contrast was computed for each subject, and all resulting contrast images were then entered into second-level random effect analyses. First, independent one-sample t-tests were performed for each methodological condition allowing to compare standard to modified pre-processing procedures and to confirm our prediction of lower geometrical distortions for the SENSE sequence by contrasting the standard and SENSE EPI sequence samples. Second, so as to directly and statistically assess the effect of the EPI-to-non-EPI non-linear registration step according to the EPI sequence samples, a 2×2 repeated-measures ANOVA including the ‘ pre-processing procedure' (including or not the EPI-to-non-EPI non-linear registration step) as a repeated factor and the EPI sequence group (standard or SENSE) as a classification factor was also performed using the SPM5 ‘Flexible factorial design' procedure.

For all these analyses, only regions surviving a False Discovery Rate (FDR)-corrected $p < .05$ threshold with an extension of at least 20 contiguous voxels were considered as significant.

Results

Observation of geometrical distortions induced by the EPI-to-non-EPI non-linear registration (Figure 2)

The jacobian determinants of the EPI-to-non-EPI non-linear registration showed that the distortion correction included expansions within the dorso-lateral frontal cortex, medial and lateral parietal areas, as well as deep gray matter nuclei, temporal poles, medial temporal lobes and anterior cingulate cortex, and contractions in the occipital, orbito-frontal, medial prefrontal, retrosplenial and lateral temporal cortices. Although slightly higher in the group with the standard sequence, the jacobians appeared highly similar in terms of location and direction (contraction or expansion) in both EPI sequence groups.

Assessment of geometrical distortions from EPI images

EPI images (colorscale) were superimposed on T1 volumes (grayscale) to compare the mismatches between these two acquisitions (and thus the degree of geometrical distortion of EPI images) before and after distortion correction (Figure 3). This display shows mismatches in the temporal poles, caudate nuclei and orbito-frontal cortex (blue arrows on Figure 3). These mismatches were found to be reduced with either the SENSE sequence or the EPI-to-non-EPI non-linear registration and all the more with both factors combined.

The effect of the EPI-to-non-EPI non-linear registration is illustrated in the native space of a single subject who underwent both EPI sequences (Figure 4), and on the two groups of subjects with different EPI sequence in the MNI space (Figure 5). Single subject displays show that, after a single rigid T1-to-EPI coregistration (as performed in the standard pre-processing procedure), the corpus callosum genu of the EPI image is located behind the corpus callosum genu of the T1 image (Figure 4 , red arrows), and relatively large distortions appear in the global shape of the parieto-occipital lobes on the EPI volume compared to the T1 image (Figure 4 , blue arrows). These two effects are lessened with either the SENSE sequence or the EPI-to-non-EPI non-linear registration and even more when both factors are combined.

Figure 5 illustrates the effect of the EPI-to-non-EPI non-linear registration for the two groups of subjects by reporting a reference point from the mean T1 image onto the EPI images of each group (red crosses). With the standard pre-processing procedure, the corpus callosum genu on the mean T1 volume (y=34) appears up to 8 mm forward (y=26) onto the mean EPI image of the group with the standard EPI sequence, and up to 4 mm forward (y=30) in the group with the SENSE EPI sequence (blue arrows). Introducing the EPI-to-non-EPI non-linear registration reduces this difference as only a 2 mm (y=32) forward gap is observed in the group with the standard EPI sequence while there is no more gap in the group with the SENSE EPI sequence (Figure 5 , blue arrows).

These visual assessments were confirmed by the ANOVA on the individual measures of the Euclidian distance between the corpus callosum genu coordinates on the EPI and that on the T1 images, which revealed a significant effect of the pre-processing procedure ($F(1,22)=26.91$, $p< .001$). The effect of the EPI sequence group ($F(1,22)=2.35$, $p> .1$), and the interaction between EPI sequence group and pre-processing procedure, failed to reach significance ($F(1,22)=0.26$, $p> .6$) (Figure 6). Quantitatively, the mean Euclidian distance between the position of the corpus callosum genu on the EPI and that on the T1 images dropped from 5.97 (±2.39) mm to 2.77 (±1.33) mm for the group with the standard EPI sequence and from 5.08 (±1.54) mm to 2.45 (±1.20) mm for the group with the SENSE EPI sequence after the EPI-to-non-EPI non-linear registration (Figure 6). To assess the reliability of this measure, the coordinates were measured a second time by the same rater. The mean Euclidian error distance between the two measures was 1.11 (±1.06) mm for T1 volumes and 1.59 (±1.24) mm for EPI volumes which is inferior to the in-plane resolution of the images used for these measures ($2\times2mm^2$).

Assessment of geometrical distortions from activation maps

Figure 7 illustrates one-sample t-tests representing main effects of the EPI sequence group and the pre-processing procedure from group analyses projected onto corresponding T1 and EPI images. This Figure shows, first, some activations located onto the corpus callosum genu after anatomical rendering onto the T1 when using the standard pre-processing procedure, while they are correctly rendered onto anterior cingulate cortex of the T1 anatomical image when introducing the EPI-to-non-EPI non-linear registration step. Second, effects of EPI-to-non-EPI non-linear registration appear increased for the group with the standard EPI sequence compared to the group with the SENSE EPI sequence.

Finally, the voxel-based ANOVA revealed a significant effect of the pre-processing procedure while no voxel reached significance for the main effect of the EPI sequence group or for the interaction between the EPI sequence group and the pre-processing procedure. Post-hoc comparisons between standard and modified procedures more specifically pointed, mainly, to increased activations into the corpus callosum genu and anterior cingulate gyrus using the standard procedure, while the modified procedure led to significantly higher activation in the medial part of the superior frontal gyrus (see Figure 8). Note that differences were also observed in smaller and less significant clusters, with decreased activations with the modified compared to the standard procedure in a very anterior part of the temporal pole and the right lateral parietal cortex and increased activations in a more posterior part of the temporal pole (Figure 8).

Discussion

The objective and quantitative assessment of geometrical distortions of EPI images is a complex issue. In the present study, the comparison of the degree of image distortion between different conditions was based on both visual assessment and quantitative measurement. First, we simply visually assessed the location and direction of the distortions induced by the method proposed in this study to correct for EPI geometrical distortions (Figure 2). Second, we used both individual and group displays illustrating the mismatches between anatomical and functional data reflecting the degree of distortions that can occur individually (as for the parieto-occipital lobes on Figure 4) on the one hand, and on group findings on the other hand (Figures 3 , 5 and 7). Third, we used the differences between the position of the corpus callosum genu on the T1 image and that on the EPI images as a quantitative measure of these mismatches. Finally, we also performed statistical analyses onto these measures so as to provide statistical insights onto geometrical distortion effects (Figures 6 and 8).

As expected, the group with the standard EPI sequence showed the highest geometrical distortions, as indicated by the degree of parieto-occipital distortions (Figure 4), of temporal pole and deep gray matter mismatches (Figure 3) and by the difference between the corpus callosum genu position on EPI and that on T1 images (Figures 4 , 5 , 6 and 7). Consistently, the standard EPI sequence also appeared to be more sensitive to the EPI-to-non-EPI non-linear registration (Figures 2 and 7), indicating higher differences between EPI and non-EPI T2 Star images and thus greater distortions. Nonetheless, no statistically significant effect of the EPI sequence group was found in our analyses which may arise from our limited sample sizes.

The EPI-to-non-EPI non-linear registration was found to strongly reduce the geometrical distortions for both EPI sequence groups. Indeed, this procedure decreased parieto-occipital distortions (Figure 4), mismatches between T1 and EPI images in temporal poles and deep gray matter nuclei (Figure 3) and the gap in the corpus callosum genu position onto EPI and T1 images (Figures 4 , 5 , 6 and 7). More specifically, the gap was found to be quantitatively lowered by about 50 percent after EPI-to-non-EPI non-linear registration for both groups with the standard and SENSE EPI sequences (Figure 6), and this reduction was found to be statistically significant. The effect of EPI-to-non-EPI non-linear registration was also visible on anterior cingulate activations: these activations overlapped the corpus callosum of the T1 using the standard procedure while they accurately matched the anterior cingulate gyrus of the T1 with the modified procedure (Figure 7). Finally, the voxel-based ANOVA on activation maps revealed significant activation decrease in the corpus callosum genu after the EPI-to-non-EPI non-linear registration, while a significant increase was observed into the most anterior part of the frontal lobe. This result provides statistical insight on the mislocation of anterior cingulate and medial-prefrontal EPI activations onto the T1 image when using the standard pre-processing procedure (Figure 8). The effects found in the same analysis within the temporal pole and lateral parietal cortex are consistent with the anatomical mismatches observed in these two regions (Figures 3 and 4). Altogether these results highlight both the efficiency of the EPI-to-non-EPI non-linear registration to correct for EPI geometrical distortions, providing improved matching between anatomical and functional MRI data, and its robustness over different EPI sequences.

The method proposed here, instead of calculating distortion maps as in the ‘FieldMap’ procedure7 ,8 , roughly corrects the distorted EPI images according to their theoretical undistorted global shape provided by the non-EPI T2 star image. Thus, even if it may not fully remove the geometrical distortions since it does not rely on an accurate measure of these distortions, our procedure appears as an efficient alternative, that may notably prove to be useful if the ‘FieldMap’ method fails to provide correct field map estimation (e.g. in cases of noisy acquisitions with unusable phase images leading to incorrect field map estimation) or if field maps have not, or cannot, be collected. Indeed, the SPM Normalize algorithm is designed to be as independent as possible to the type and noise properties of the images18 and the degree of freedom of the algorithm was not found to influence the distortion correction through this method (data not shown). Moreover, this non-linear registration procedure is both fast and easy to implement as it simply relies on Normalize algorithms, which are widely

implemented in brain analysis software, and acquisition of a single non-EPI T2 Star volume, which only lasted three minutes in the present study. Note that we did not specifically assess the effects of using different Normalize algorithms here, although the lack of significant influence of the number of degrees of freedom suggest they would be minimal.

EPI geometrical distortions are in-plane and in one direction (the phase encoding direction), and contrary to the 'FieldMap' procedure, the calculated warps with the method proposed here can be out of plane and in any direction. Hence, the use of in-plane non-linear registration algorithms could help to deal with that limitation and would improve this method. Nevertheless, visual assessments of the warps induced by our correction method showed no evidence of aberrant distortion corrections (Figures 2 , 3 , 4 , 5 and 7).

Finally, distortion correction was also found to have an effect on other brain structures, such as the medial temporal and the occipital lobes (see Figure 2). We failed to provide quantitative information onto the degree of distortion and the effect of correction for other brain location than the corpus callosum genu (see Materials & Methods), which is a limitation of the current study. However, yet only based on visual/qualitative assessment, our findings in the medial temporal and the occipital lobes further reinforce the relevance of distortion correction for fMRI paradigms involving these areas.

As a conclusion, these findings altogether provide strong evidence for the effectiveness of the EPI-to-non-EPI non-linear registration to decrease geometrical distortions of EPI images, and thus to improve anatomical accuracy of EPI-based fMRI results. While more sophisticated methods might prove to be more accurate, this method is interestingly very simple, easy to implement and widely available. Thus, the EPI-to-non-EPI non-linear registration procedure, is an easy way to improve the anatomical accuracy of fMRI results labelization and interpretation, and may be useful for current and future research challenges.

Ackowledgements:

Funding Source: ANR (Agence Nationale de la Recherche, Longévité et Vieillissement, 2007), Inserm, including Inserm-Liliane Bettencourt MD-PhD Program and Région Basse-Normandie.

We acknowledge the financial/scientific support of the ANR (Agence Nationale de la Recherche, Longévité et Vieillissement, 2007), Inserm, including Inserm-Liliane Bettencourt MD-PhD Program and Région Basse-Normandie for this project. We are grateful to the two anonymous reviewers for their helpful comments regarding this manuscript. We thank R. La Joie and C. Duval for their time and help in preliminary tests of the fMRI paradigm, F. Lamberton and N. Delcroix for their help with the EPI sequences and the aborted FieldMap corrections, F. Mézenge and A. Pélerin for help with recruitment of subjects, G. Perchey and M.H. Noël for help with neuroimaging data acquisition, and the volunteers of this study.

Footnotes:

No conflict of interest to disclose.

References:

- 1 . Margulies DS , Kelly AM , Uddin LQ , Biswal BB , Castellanos FX , Milham MP . Mapping the functional connectivity of anterior cingulate cortex . Neuroimage . 2007 ; 37 : 579 - 588
- 2 . Zeineh MM , Engel SA , Thompson PM , Bookheimer SY . Dynamics of the hippocampus during encoding and retrieval of face-name pairs . Science . 2003 ; 299 : 577 - 580
- 3 . Vigneau M , Beaucousin V , Herve PY , Duffau H , Crivello F , Houde O , Mazoyer B , Tzourio-Mazoyer N . Meta-analyzing left hemisphere language areas: phonology, semantics, and sentence processing . Neuroimage . 2006 ; 30 : 1414 - 1432
- 4 . Vanderwal T , Hunyadi E , Grupe DW , Connors CM , Schultz RT . Self, mother and abstract other: an fMRI study of reflective social processing . Neuroimage . 2008 ; 41 : 1437 - 1446
- 5 . Chételat G , Desgranges B , Landeau B , Mezenge F , Poline JB , de la Sayette V , Viader F , Eustache F , Baron JC . Direct voxel-based comparison between grey matter hypometabolism and atrophy in Alzheimer's disease . Brain . 2008 ; 131 : 60 - 71
- 6 . Casanova R , Srikanth R , Baer A , Laurienti PJ , Burdette JH , Hayasaka S , Flowers L , Wood F , Maldjian JA . Biological parametric mapping: A statistical toolbox for multimodality brain image analysis . Neuroimage . 2007 ; 34 : 137 - 143
- 7 . Hutton C , Bork A , Josephs O , Deichmann R , Ashburner J , Turner R . Image distortion correction in fMRI: A quantitative evaluation . Neuroimage . 2002 ; 16 : 217 - 240
- 8 . Cusack R , Brett M , Osswald K . An evaluation of the use of magnetic field maps to undistort echo-planar images . Neuroimage . 2003 ; 18 : 127 - 142
- 9 . Kjaer TW , Nowak M , Lou HC . Reflective self-awareness and conscious states: PET evidence for a common midline parietofrontal core . Neuroimage . 2002 ; 17 : 1080 - 1086
- 10 . Macrae CN , Moran JM , Heatherton TF , Banfield JF , Kelley WM . Medial prefrontal activity predicts memory for self . Cereb Cortex . 2004 ; 14 : 647 - 654
- 11 . Craik JIM , Moroz TM , Moscovitch M , Stuss DT , Winocur G , Tulving E , Kapur S . In Search of The Self: a Positron Emission Tomography Study . Psychol Sci . 1999 ; 10 : 26 - 34
- 12 . Johnson SC , Baxter LC , Wilder LS , Pipe JG , Heiserman JE , Prigatano GP . Neural correlates of self-reflection . Brain . 2002 ; 125 : 1808 - 1814
- 13 . Ries ML , Schmitz TW , Kawahara TN , Torgerson BM , Trivedi MA , Johnson SC . Task-dependent posterior cingulate activation in mild cognitive impairment . Neuroimage . 2006 ; 29 : 485 - 492
- 14 . Wager TD , Nichols TE . Optimization of experimental design in fMRI: a general framework using a genetic algorithm . Neuroimage . 2003 ; 18 : 293 - 309
- 15 . Ashburner J , Friston KJ . Unified segmentation . Neuroimage . 2005 ; 26 : 839 - 851
- 16 . Villain N , Desgranges B , Viader F , de la Sayette V , Mezenge F , Landeau B , Baron JC , Eustache F , Chételat G . Relationships between hippocampal atrophy, white matter disruption, and gray matter hypometabolism in Alzheimer's disease . J Neurosci . 2008 ; 28 : 6174 - 6181
- 17 . Poline JB , Worsley KJ , Holmes AP , Frackowiak RS , Friston KJ . Estimating smoothness in statistical parametric maps: variability of p values . J Comput Assist Tomogr . 1995 ; 19 : 788 - 796

- 18 . Ashburner JT , Friston KJ . Editor: Friston KJ , Ashburner JT , Kiebel SJ , Nichols TE , Penny WD . Non-linear Registration . Statistical Parametric Mapping - The Analysis of Functional Brain Images . 1 Amsterdam Elsevier ; 2007 ; 63 - 80

Figure 1

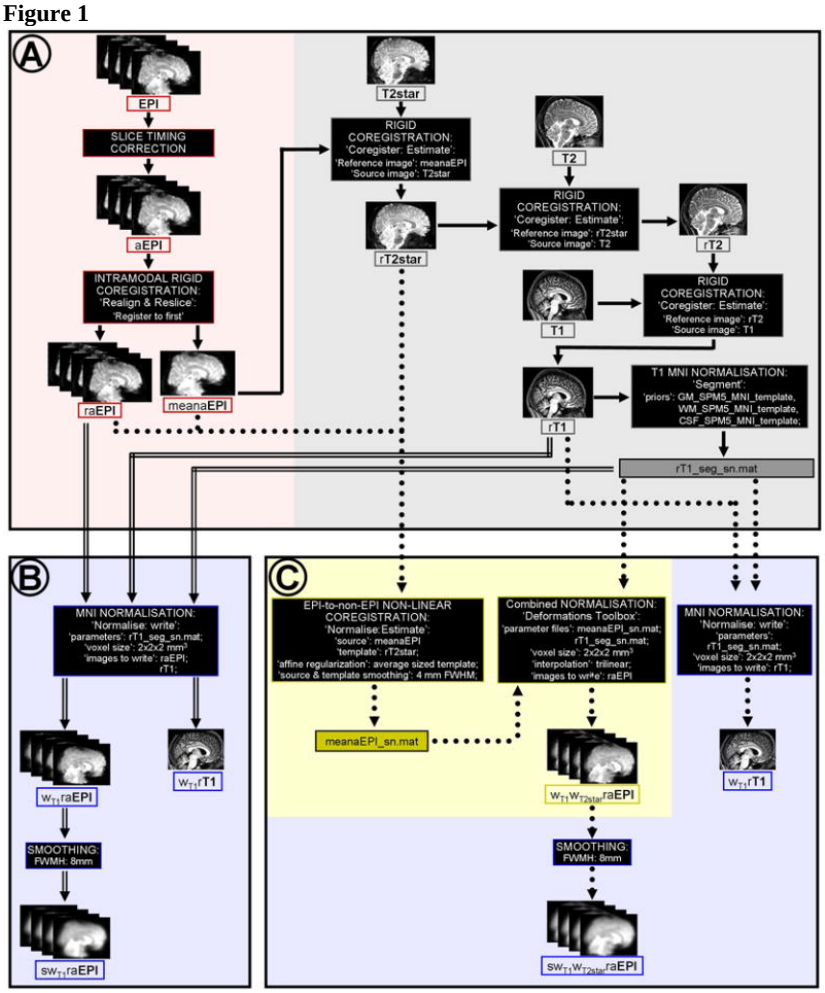

Figure 2

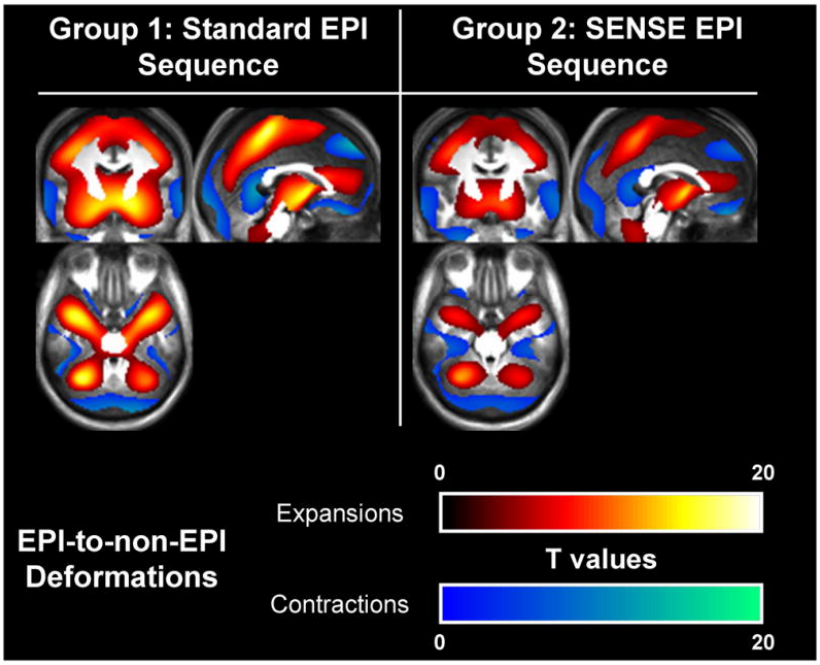

Figure 3

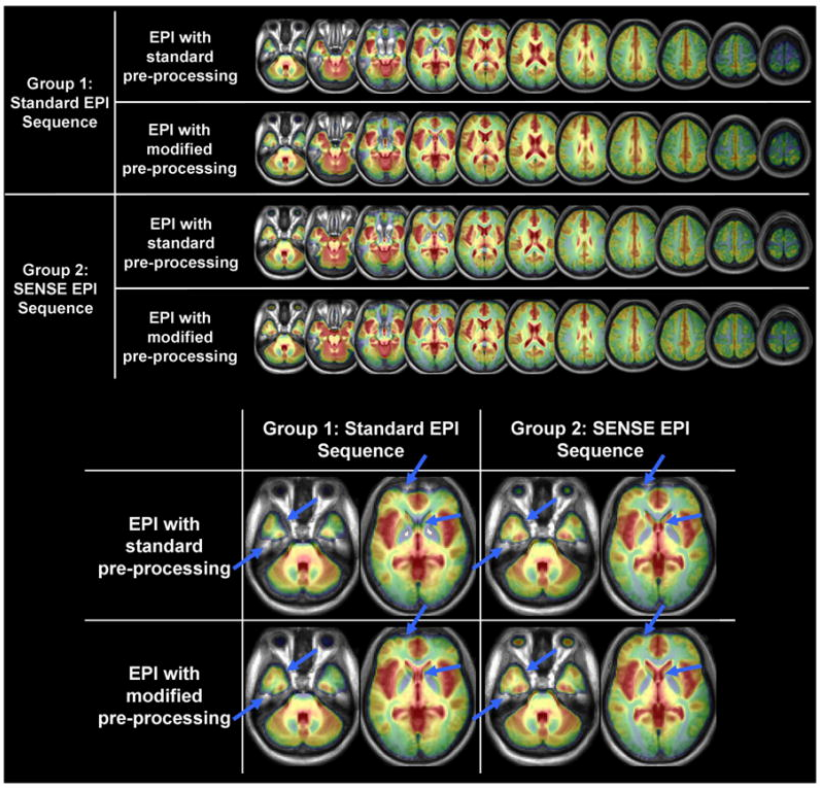

Figure 4

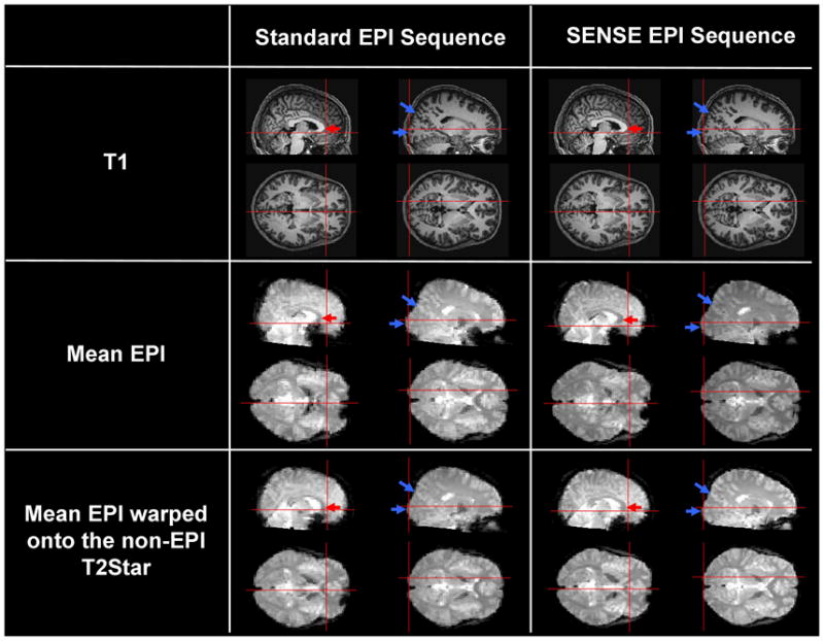

Figure 5

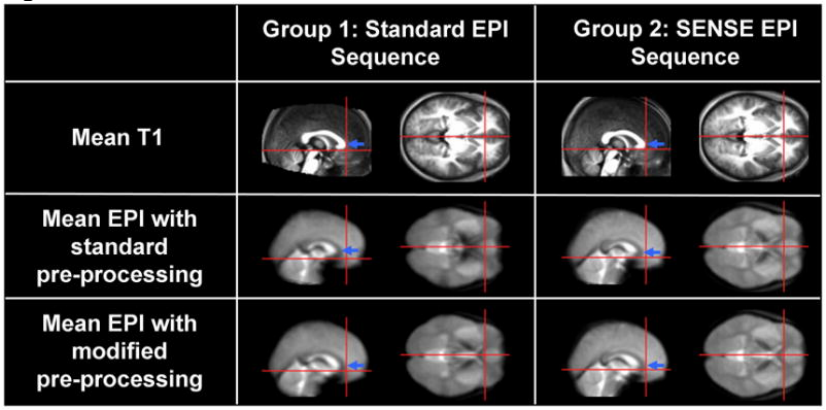

Figure 6

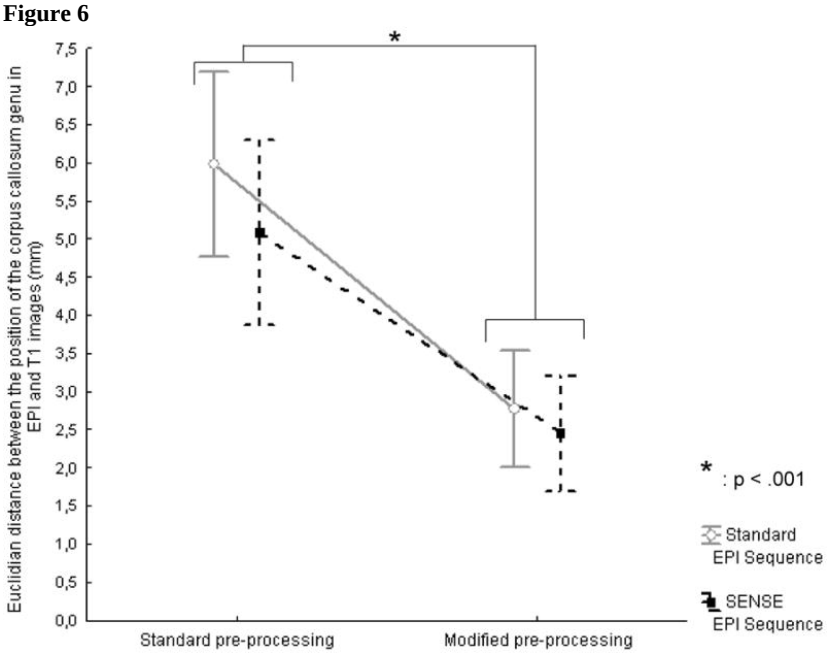

Figure 7

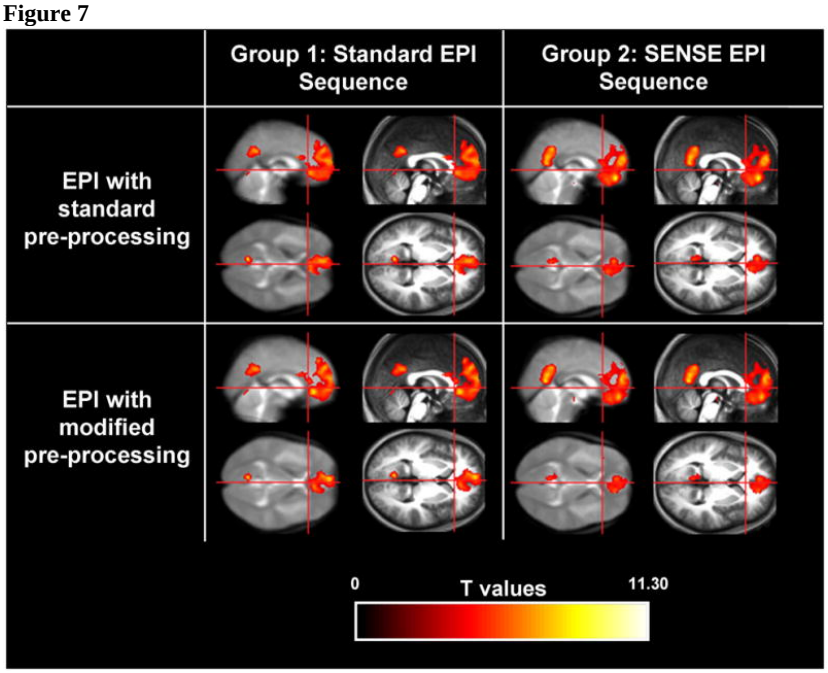

Figure 8